Flood drivers and trends: a case study of the Geul River Catchment (the Netherlands) over the past half century

Athanasios Tsiokanos[1,2], Martine Rutten[1], Ruud J. van der Ent[1], and Remko Uijlenhoet[1]

[1]Department of Water Management, Faculty of Civil Engineering and Geosciences, Delft University of Technology, Delft, The Netherlands
[2]Department of Catchment and Urban Hydrology, Unit of Inland Water Systems, Deltares, Delft, The Netherlands

Correspondence: Athanasios Tsiokanos (Athanasios.Tsiokanos@deltares.nl)

Abstract. Extreme precipitation in July 2021 caused devastating flooding in Germany, Belgium and in the Netherlands, particularly in the Geul river catchment. Such precipitation extremes were not recorded previously and were not expected to occur in summer. This contributed to poor flood forecast and hence to large damage. Climate change was mentioned as a potential explanation for these unprecedented events. Yet, before such a statement can be made, we need a better understanding of the

5 drivers of floods in the Geul and their long-term variability, which are poorly understood and have not been examined recently. In this paper, we use an event-based approach to identify the dominant flood drivers in the Geul and employ a multi-temporal trend analysis to investigate their temporal variabilities, as well as, a novel methodology to detect the dominant direction of a trend. Results suggest that extreme 24-hour precipitation cannot solely lead to floods. Heavy multi-day precipitation is the primary high-flow driver in the catchment and the joint probability of heavy and prolonged rainfall with wet initial conditions

10 (compound event) determines the chances of flooding. Critical precipitation (precipitation that leads to floods) shows a consistent increase in the winter half-year, a period in which more than 70% of extremely high flows have occurred historically. While no consistent trend patterns are evident in the majority of precipitation and extreme flow trends in the summer half-year, an increasing direction in the recent past is visible.

1 Introduction

15 In July 2021, Western Europe was struck by unprecedented precipitation, leading to disastrous flooding in Germany, Belgium, and the Netherlands (Journée et al., 2023; Kreienkamp et al., 2021). This event ranked among the most devastating natural disasters to hit Europe in the past 50 years, resulting in a minimum of 220 deaths and causing an estimated economic damage of approximately EUR 46 billion (MunichRe, 2022; Mohr et al., 2023). In the Netherlands, the Geul river catchment (344 km[2]) was the most impacted, where the economic damage of the floods was estimated to exceed EUR 200 million, constituting

20 approximately 50% of the total estimated damage in the country (Task Force Fact Finding hoogwater 2021, 2021). The event revealed weaknesses in flood risk management. Flood risks were poorly communicated to the inhabitants (Slager, 2023). The flood forecasting system for the Geul was under maintenance, and even if it had been operational, predictions would not have been accurate, because of poor representation of flood-generating processes according to the responsible authorities (Task Force Fact Finding hoogwater 2021, 2021). The Geul catchment is considered quite an exceptional and atypical catchment

25 for the Netherlands due to its steep topography (elevations range from 40 to nearly 400 m) and deep soils (tens of meters). A proper understanding of flood drivers in the area is considered an important stepping-stone in mitigating the risks in the future.

Floods in a catchment are caused by the interaction of meteorological, river system, and catchment characteristics (Andrés-Doménech et al., 2015). Hydrological catchment properties can regulate streamflow response (Sharma et al., 2018), for example, extreme precipitation does not always result in floods in various basins around the world (Wasko and Nathan, 2019;
30 Nanditha and Mishra, 2022; Berghuijs et al., 2019). Among the catchment characteristics, antecedent conditions (e.g., soil moisture) can play a crucial role in driving high flows (Bertola et al., 2020; Woldemeskel and Sharma, 2016). Many locations around the world have seen the effects of wet antecedent conditions on flood risk (e.g., Garg and Mishra, 2019). Especially in lowland catchments the discharge response can be strongly influenced by the catchment wetness, due to shallow groundwater and its effects on rainfall flow paths (Brauer et al., 2018). As a result, determining the relative contribution of antecedent
35 wetness conditions and extreme precipitation in causing high river flows is critical.

The identification of the drivers of observed flood events has received increasing attention in the recent literature (e.g., Blöschl et al., 2019; Bertola et al., 2020). Examining relations between trends or seasonality in flood peaks and factors such as extreme precipitation or soil moisture to define flood drivers is well established (Blöschl et al., 2019; Do et al., 2017; Tramblay et al., 2021; Wasko et al., 2020). However, to enhance our knowledge of flood dynamics, an event-based approach
40 has been suggested (Nanditha and Mishra, 2022; Tramblay et al., 2021; Berghuijs et al., 2019). This approach entails identifying the specific drivers behind individual flood events or extremely high-flow occurrences. By analyzing the characteristics and circumstances surrounding these events, one can gain valuable insights into the mechanisms and factors that contribute to their intensity and occurrence (Nanditha and Mishra, 2022).

A proper understanding of flood drivers does not only include their identification but also their long-term change. Investi-
45 gating the changes of variables that can cause a hazard is crucial for managing the risks in an effective way (Yang et al., 2021) and can facilitate the planning of reliable and meaningful interventions. Making a critical assessment of the past and current states and providing the long-term trends of hydroclimatic variables play a key role in future projections (Squintu et al., 2021). Trends and changes in the time series of hydrological and climatological data have received attention in catchments and areas across the world (e.g., Blöschl et al., 2017; Do et al., 2017; Hannaford et al., 2021; Murphy et al., 2020).

50 However, most of the existing trend tests are limited, as they are conducted within fixed timeframes, which may fail to accurately capture the historical variability. The significance and magnitude of trends can vary considerably based on the chosen study period and duration. To deal with this limitation, multi-temporal trend approaches have been leveraged (e.g., Hannaford et al., 2021; Murphy et al., 2020), considering all possible combinations of start and end-year periods. Although these analyses have helped in the identification of temporal variabilities, a research gap remains in determining the main trend
55 direction, such as consistency or stability, across all studied time frames. Lupikasza (2010) developed criteria for expressing trend stabilities using a fixed 30-year moving window, however, this approach did not fully consider the entire variability (multi-temporal analysis) but instead utilized an overlapping period which can be misleading. Since each 30-year window overlaps with the previous and subsequent windows, trends can be missed or misinterpreted because the overlapping periods could obscure them. Using only overlapping periods can lead to artificially smooth trends not representing the true (long-term)

60 variability of the data. In addition, the length of the selected moving window might introduce bias in the analysis. Trends over longer periods and with different combinations of start and end-year periods expressing the full historical variation should be also taken into account in the calculation of the main direction. To address these limitations, our study aims to develop a methodology that can identify and assess trend consistency in multi-temporal analysis, taking into account the complete range of variability.

65 In summary, the Geul river catchment consists an interesting example of a hilly catchment in northwest Europe, with unique hydrological characteristics that are shaped by the underlying geology, topography and land use. The recent floods have shown that there is a need for further research into the drivers of flooding in the area, particularly in the context of climate change. Specifically, the role of extreme precipitation and antecedent conditions as potential flood drivers and their long-term variability remain to be examined. In this paper, we address the following scientific questions that are crucial for our understanding of

70 floods in the Geul River catchment: (a) *What are the dominant flood drivers in the Geul river catchment in different seasons?* and (b) *What are the trends (temporal variability and consistency) of the critical precipitation and extreme discharges in the catchment?* To identify the dominant flood drivers we use an event-based approach. In addition, we utilize a multi-temporal trend analysis to investigate the temporal variabilities of the trends and we develop a new methodology to detect the dominant direction (i.e. consistency) of a trend.

2 Methods and materials

75

2.1 Study area

The Geul river is an important tributary of the Meuse and is located in the Netherlands, Belgium, and part of Germany, close to the three-border region (Fig. 1). The total area of the Geul catchment is approximately 344 km^2. The Geul drops about 250 m over approximately 60 km, making it one of the few steeply sloping rivers in the Netherlands. The Geul river has an

80 average discharge of approximately 3.2 m^{3}s^{-1} (at the outlet of the catchment) and is mainly rain-fed. As a consequence, its discharge can change dramatically during flood and drought events (e.g. ranging from 1 m^{3}s^{-1} during drought periods to more than 40 m^{3}s^{-1} during floods). The response time of the catchment is in the order of one to two days (Asselman et al., 2022). The annual average precipitation is approximately 870 mm yr^{-1} and is rather uniformly distributed over the year (see Fig. 2a). Average annual discharge at the outlet of the catchment and potential evaporation are about 307 mm yr^{-1} and 585 mm

85 yr^{-1} respectively, based on time series from 1970 to 2021. The flow regimes in the Geul do not show large variations (Fig. 2). The, on average, rather equal distribution of runoff in the Geul throughout the year is due to the effect of groundwater storage provided by large chalk aquifers in the catchment (Tu, 2006). The long-term evaporative index is approximately 0.67 and the runoff ratio 0.35.
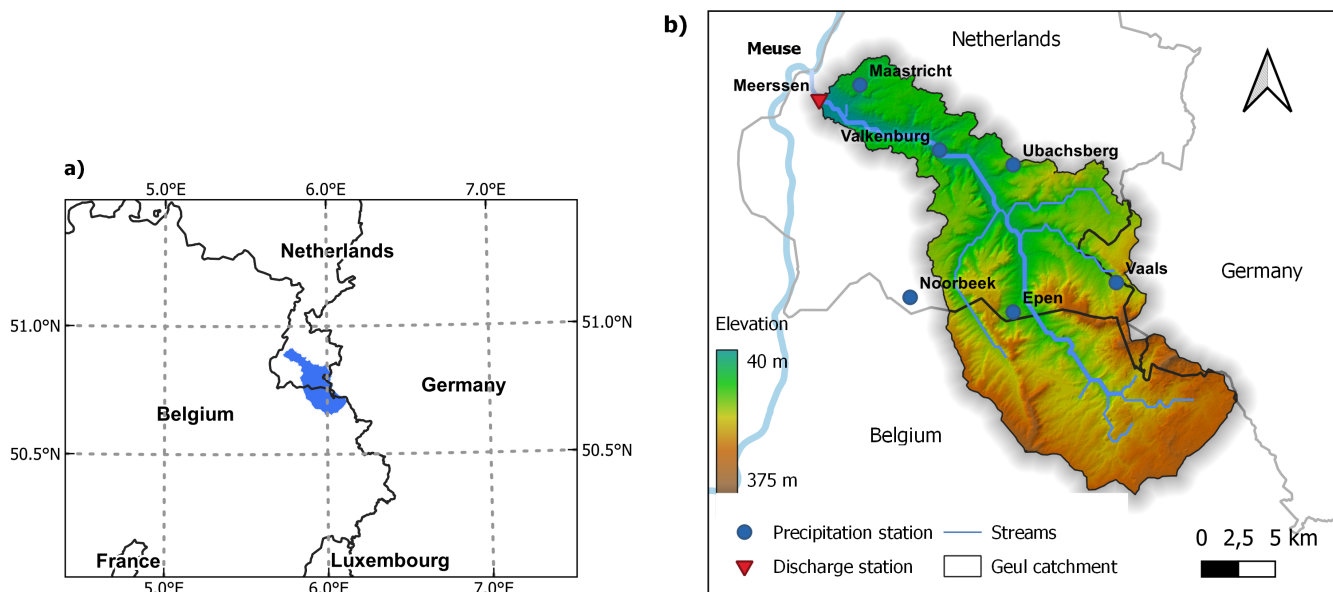
Figure 1. (a) Location of the Geul river catchment (blue shaded area), (b) elevation map of the study catchment including the location of precipitation stations and the discharge observation station at the outlet.
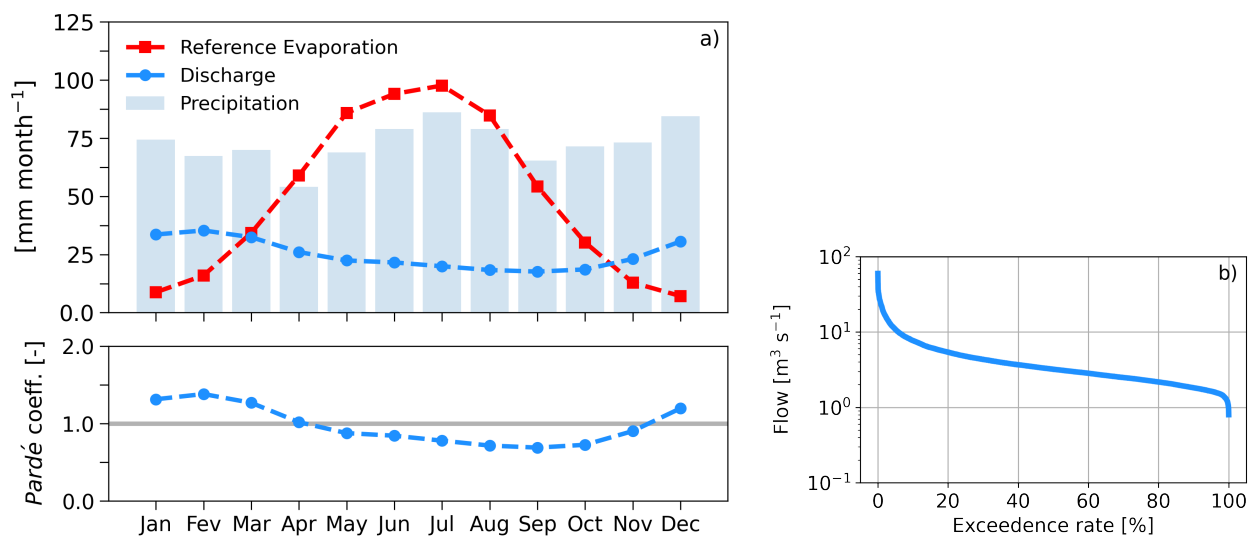
Figure 2. (a) Upper panel: Monthly averages for precipitation (averaged using Thiessen polygons), reference (Makkink) evaporation (obtained from the Maastricht meteorological station) and discharge in the Geul catchment, Lower panel: Flow regimes of the Geul based on Pardé coefficient, defined as the ratio of the average monthly discharge to the average annual discharge, (b) Flow duration curve along the Geul based on the mean daily discharge. All graphs are produced using time series from 1970 to 2021.

2.2 Data sets

90 Streamflow time series at the outlet of the catchment (station Meerssen), were made available by the local water authority Waterschap Limburg, including 15-minute measurements from 1970 up to August 2021. From 1970 to 2011 measurements were taken using a measuring weir, while since 2011 discharges are measured using Acoustic Doppler Current Profilers (ADCP) (van der Deijl, 2023). Historical flood event data (i.e. date of occurrence) are based on Thewissen (2022), who performed a local newspaper search using Delpher, a Dutch database containing digitized texts from newspapers, books, and magazines.

95 These collections are curated by scientific organizations, libraries, and heritage institutions. Thewissen (2022) obtained the data through an iterative process that involved Optical Character Recognition (OCR) and manual scanning. In this research, a flood is defined as surpassing the bankful capacity. For detailed information about the search methodology, please refer to Thewissen (2022).

Records of 24-hour precipitation from five stations located in (or near) the Geul river catchment are used (see Fig. 1).

100 The data used in this study come from the Royal Netherlands Meteorological Institute (KNMI) manual rain gauge network. Volunteer observers operate the rain gauges on a 24-hour basis (from 8 am to 8 am local time). In addition to the volunteer KNMI stations, daily (calendar days) measurements from the automated meteorological station at Maastricht are used. Data from automated stations are also available at an hourly basis, however the daily scale is used in order to have the same resolution for each station. The time series are complete (except for three missing months at Noorbeek) and are considered to be of high

105 quality, as KNMI performs regular quality tests (Buishand et al., 2013). Days with extremes were checked and it was found that all of them occurred during well-known high precipitation or flood events.

The available precipitation record periods slightly differ between the selected stations and mainly start in the 1950s, except the new Epen station, which has a record from 1981 onward. Specifically, stations at Vaals, Valkenburg, and Noorbeek have a record from 1951 onward, while the available time series at the Maastricht and Ubachsberg stations start from 1958 and 1955,

110 respectively. Due to its shorter available period the station Epen is excluded from the analysis. The precipitation stations located in the uppermost regions of the catchment in Belgium were not taken into account due to their limited temporal coverage, lack of alignment with the discharge (and the KNMI data), and unsuitability for trend analysis.

Another important factor to consider when analyzing meteorological time series, and especially trends, is data (in)homogeneity. Trends represent the long-term changes in the data over time caused by natural/climate variability, while inhomogeneities rep-

115 resent changes in the data that are not part of the underlying trend. There are several types of modifications that can occur and can cause significant non-climatic alternations (inhomogeneities) in the data, especially in long time series, such as changes in the location of the measuring station, differences in the manner and the procedures (e.g. measuring frequency) or changes in the instruments/tools. Performing statistical tests for homogeneity on precipitation data measured at daily frequencies is challenging or practically infeasible (Lupikasza, 2010). This can be attributed to the fact that daily time series show strong

120 random variations. For this reason, the precipitation time series were aggregated to monthly sums and then tested using two well-known homogeneity tests: the Standard Normalised Homogeneity Test (SNHT) (Alexandersson, 1986; Alexandersson

and Moberg, 1997) and Buishand's U test (Buishand, 1984). Both tests were applied at a significance level of 5% (α=0.05). The test results showed that the data time series were free of significant errors and no inhomogeneities were detected.

2.3 Flood driver detection

125 #### 2.3.1 Extreme indicators

Hydrological years are used instead of calendar years to ensure a more accurate representation of the frequency and intensity of extreme events that may occur within a particular hydrological regime. Similarly to Tu (2006) and Sperna-Weiland et al. (2015), we define a hydrological year from November to October, for the study area. Half-year hydrological winter (from November to April) and summer (from May to October) are also considered.

130 Two types of flood data time series are used: annual maxima (denoted as Q_{max}), including winter and summer yearly maxima (denoted as $Q_{\mathrm{W,max}}$ and $Q_{\mathrm{S,max}}$, respectively), and extremely high flows using the peaks over threshold (POT) method (Haan, 2002). The maximum daily discharge is extracted from the 15-min discharge data and hydrological years with over 20% missing daily values are omitted from the analysis. Consequently, the years 1971, 1974, and 1990 have been excluded from the Q_{max} times series. For identifying extremely high flows we use the 99th percentile threshold (Nanditha and Mishra, 2022;

135 denoted as Q_{99}) extracted from the maximum daily discharge time series from 1970 to 2021, excluding daily missing values. We use only extremely high events separated by a time frame of five days to ensure that the selected high flows are independent and do not belong to the same flood wave.

Floods are generally caused by a combination of initial moisture conditions and precipitation. To explore the probable causes of high flow episodes, we employ six indicators to assess precipitation and antecedent soil moisture levels: extreme precipitation

140 (denoted as P_{99}), multi-day precipitation (denoted as P_{MD}), wet antecedent conditions (denoted as P_{WAC}), P_{99} combined with P_{WAC} (denoted as Compound I), P_{MD} combined with P_{WAC} (denoted as Compound II), and P_{99} and P_{MD} combined with P_{WAC} (denoted as Compound III). We estimate P_{99} as the events that exceed the 99th percentile of wet days (days with more than 1 mm precipitation). We define P_{MD} events, using the 95th percentile threshold (Nanditha and Mishra, 2022) of the all-4day accumulated (rolling sum) precipitation, considering the hydrological functioning of the catchment (Asselman et al.,

145 2022). With a 4-day duration, we want also to ensure that the 95th percentile used for a P_{MD} event is higher than the 99th percentile used for an P_{99} event. In this way, the distinction between P_{MD} and P_{99} becomes clearer. As a P_{MD} event cannot cause a P_{99} event, we expect that usually more than 24 hours of precipitation are needed to cause P_{MD}. This is not always the case as in very extreme events the 24-hour precipitation can cause at the same time P_{99} and P_{MD} which is unavoidable. The sensitivity of the results to the duration of a P_{MD} event is further discussed in Sect. 3.1.1. In addition, the P_{MD} definition

150 allows the assumption that P_{MD} can be used as a proxy of heavy prolonged rainfall. Furthermore, we use the Antecedent Precipitation Index (ratio of 30-day pre-event precipitation to long-term average for the same period; API) as developed by Marchi et al. (2010), to access the initial catchment conditions and get an estimate of the initial (soil) conditions. Marchi et al. (2010) classifies antecedent moisture conditions as follows: (1) dry: $0 < \mathrm{API} \leq 0.5$; (2) normal: $0.5 < \mathrm{API} \leq 1.5$; and (3) wet: API > 1.5. P_{WAC} corresponds to API values higher than 1.5 (Marchi et al., 2010).

2.3.2 Monthly distribution of extremes

In order to get a rough indication of the effects of extreme rainfall on high flows, we estimate the monthly distribution of P_{99}, P_{MD}, annual maximum precipitation (denoted as P_{max}) and high flow extremes (i.e. Q_{99} and Q_{max}), together with the past flood events (denoted as FE). Despite the fact that the monthly distribution of P_{WAC} events cannot be directly related to the monthly distribution of high flow extremes, as P_{WAC} indicate wetter than average conditions any time of the year, their relative frequencies can provide useful insights. For this reason, we also calculate the monthly frequencies of P_{WAC}. To achieve this each, daily timestep in the precipitation series is treated as an individual event. This involves summing the precipitation amount for each day over the previous 30 days and then dividing this sum by the 30-day long-term average for the same period across the entire time series. In this way, an API index per day is obtained.

The use of all-day percentiles for discharge (Q_{99}) and wet-day percentiles for rainfall (P_{99}) may lack statistical robustness, primarily because there could be a potential increase in the number of wet days over the study period (Schär et al., 2016). To address the potential issue a trend test in the number of wet days per year and station was conducted using the non-parametric Mann-Kendall (M-K) (Kendall, 1955; Mann, 1945) test at a significance level of 0.05. The analysis did not reveal any significant trends in the number of wet days.

2.3.3 Event-based analysis

After the seasonal assessment of the extreme indicators and high-flow events, an event-based approach is followed to detect the predominant flood driver(s) in the catchment. Specifically, we calculate the likelihood of the six precipitation indicators (i.e., P_{99}, P_{MD}, P_{WAC}, Compound I, Compound II and Compound III) preceding selected high flow episodes (i.e. Q_{max}) in order to determine the primary flood cause. We use the Q_{max} events instead of the Q_{99}, as they are better defined for identifying flood drivers including all major flood events, considering also that the P_{99} is calculated from a significantly longer data series than the Q_{99}. We conduct a comprehensive analysis of each high-flow event, examining the frequency of occurrence for each indicator before a Q_{max} event. Specifically, we determine how many times an indicator occurred in relation to the total number of Q_{max} events, effectively calculating its likelihood in contributing to such occurrences. The six indicators used in this paper help examine the relative role of extreme precipitation, prolonged heavy rainfall, extreme soil moisture conditions, and compound extremes in generating high flows. For instance, if P_{99} is the main flood cause in the catchment, then P_{99} is highly likely to occur during the duration of the flood (precipitation amount of the same day) or within one day before the commencement of the event. Here, we use a two-day interval (i.e. precipitation at the same or the previous day of the flood event) for mainly two reasons: (a) the lag time of the catchment and (b) to eliminate errors due to the use of daily values (e.g., a high flow event may occur early morning due to P_{99} from the previous day).

As we directly compare the likelihood of each indicator leading to Q_{max}, it is important to note that the comparison among different flood drivers may be affected by the rarity of certain events. The total number of flood indicators varies, particularly for the most extreme ones, such as P_{99}, Compound I, and Compound III. For instance, in some years, a P_{99} event might not occur, and therefore, it cannot precede Q_{max}. To account for this effect, the reverse scenario is also considered: given that a

driver has occurred, what is the relative frequency of it being followed by a $Q_{\max}$ event. Thus, we calculate the number of unique hydrological years in which a driver is observed and determine how often $Q_{\max}$ is also observed within these instances.

190 Additionally, we provide general information about the frequency of the different drivers occurring, regardless of whether $Q_{\max}$ has occurred.

Antecedent catchment wetness and precipitation depths are crucial factors for floods in terms of magnitudes and volumes. In addition to the aforementioned flood indicators, we delve deeper into this relationship by employing the nonparametric Spearman's rank-order correlation method to correlate the half-year maximum discharge time series ($Q_{\mathrm{W,max}}$ and $Q_{\mathrm{S,max}}$)

195 with their k-day antecedent precipitation depth (denoted as P_{kD}, where k = 1, 3, 5, 7, 10, 15, 30 and 40 days; Tu, 2006). The antecedent precipitation depths are computed by summing the precipitation on the day of the high flow event and the previous k days (Tu, 2006). Table 1 provides an overview of all the different flood indicators used in this study, along with their corresponding definitions.

Table 1. Extreme indicators used to identify the main flood drivers. The initial six indicators are used to calculate probabilities preceding high-flow episodes, whereas the last indicator is correlated with high flows

Indicator	Estimation method
Extreme precipitation (P_{99})	24-hour precipitation exceeding the 99th percentile of rainy days (more than 1 mm)
Multi-day precipitation (P_{MD})	Four-day accumulated precipitation amount exceeding the 95th percentile thresholds
Wet antecedent conditions (P_{WAC})	Antecedent Precipitation Index (API) value higher than 1.5
Compound I	Extreme precipitation occurring on wet antecedent conditions
Compound II	Multi-day precipitation occurring on wet antecedent conditions
Compound III	Extreme and multi-day precipitation occurring on wet antecedent conditions
Antecedent precipitation depths (P_{kD})	Sum of precipitation on the day of the high flow event and the previous k days

One crucial concern is the timing difference of the measured daily values, i.e. calendar days for discharges and 24-hour

200 sums from 8 UTC for precipitation. The reported time/date in the precipitation time series (for the manual rain gauge network; Valkenburg, Ubachsberg, Noorbeek and Vaals stations) is the end time of observation. For this reason, the $Q_{\max}$ time of occurrence is checked: if the time of the maximum 15-min discharge values is observed to be between 00:00 and 8:00 AM the calendar day of this event is reported, otherwise, the next day is considered as the date of occurrence of the event for the (manual rain gauge) precipitation time series. In this way, we ensure the agreement in precipitation and $Q_{\max}$ time series.

205 **2.4 Trend analysis**

The temporal variability and the trends of the aforementioned potential flood drivers (i.e. P_{99}, P_{MD} and P_{kD}) are investigated. Trends in P_{kD} are based on the annual maximum values. In contrast to the definition of P_{99} in Sect. 2.3.3, we use the 95th percentile, as events that exceed the 99th percentile are extremely rare and result in many zero values in the time series, especially in winter periods, making the trend analysis unstable. The new index is denoted as P_{95} and represents the annual

210 total precipitation from days exceeding the 95th percentile. Similarly to P_{99} the 95th percentile is calculated using the whole

range of the time series and only wet days. Finally, the P_{MD} trends are investigated by summing the annual amount of four-day accumulated precipitation that exceeds the 95th percentile thresholds (of the four-day rolling sum). The used precipitation trend indices are similar to ETCCDI (Expert Team on Climate Change Detection Indices) and have been frequently applied (Klein Tank et al., 2002; Dunn et al., 2020). The aforementioned precipitation indices are calculated for winter and summer

215   periods. In addition, trends in the half-year maximum discharges ($\mathrm{Q}_{W,max}$ and $\mathrm{Q}_{S,max}$) are examined in order to detect possible consequences of extreme precipitation on extreme streamflows. We use the non-parametric M-K test to detect significant trends. To this end, a Python package that contains all the types/modifications of the M-K test, as developed by Hussain and Mahmud (2019), is used. The modified M-K test, which accounts for the influence of serial correlation on trend calculations, is employed for the analysis of the discharge time series, while the original M-K test is applied to the precipitation indices. This selection is

220   made based on the assumption that the precipitation time series exhibit no significant serial correlation.

The statistical significance and direction of the trends in the multi-temporal approach are used in order to determine the temporal consistency of a trend for each precipitation index. We express consistency as the percentage of time (t) for which trends are statistically significant. Trends that are significant at $\alpha = 0.2$ (Łupikasza et al., 2011) are defined as statistically significant trends. Since precipitation is characterized by strong temporal and spatial variation, the statistical significance levels

225   can be lower compared to other climatic variables (Łupikasza et al., 2011). In addition, the large number of calculated trends (more than 850 for most stations) allows the use of lower significance levels for expressing stabilities or consistencies. In a multi-temporal approach, it is preferable to focus on the direction and intensity of the trends, rather than whether they surpass a strictly predetermined and somewhat arbitrary level of significance (Hannaford et al., 2013). A trend in an index is considered as inconsistent, weakly consistent, consistent and strongly consistent according to the following criteria: (1) inconsistent: 0 %

230    $< t \leq 15$ % or the number of significant increasing and decreasing trends are similar (i.e. the percentages of significant trends in the same direction ranges between 40 % and 60 %); (2) weakly consistent: 15 % $< t \leq 25$ % and more than 60 % of significant trends are in the same direction; (3) consistent: 25 % $< t \leq 45$ % and more than 60 % of significant trends are in the same direction; and (4) strongly consistent: $t > 45$ % and more than 60 % of significant trends are in the same direction.

3   Results

235 ### 3.1   Identification of the dominant flood driver

Figure 3 shows the seasonal distribution of extreme precipitation (P_{99}; 69 events - about 0.4% of the daily time series from 1970 to 2021), annual maximum precipitation ($P_{\max}$; 52 events), multi-day precipitation (P_{MD}; 933 events - 5% of the four-day accumulated time series from 1970 to 2021) and wet antecedent condition events (P_{WAC}; 2705 events - 14% of the 30-day accumulated time series from 1970 to 2021) at the Vaals station, as an example, as well as high flow events ($Q_{\max}$ and Q_{99};

240   49 and 91 events, respectively) together with past flood events (FE; 30 events) in the catchment. General information on the frequency of the flood drivers averaged for all rainfall stations, is provided in Table 2. An opposing seasonality is visible between extreme precipitation and high flow events. The relative frequencies of P_{99} and $P_{\max}$ in half-year summer periods are 75% and 73%, respectively, while these percentages are only 22% and 29%, for the $Q_{\max}$ and Q_{99} events. This pattern is also

verified by the past flood events: only 26% of them occurred during half-year summers. P_{MD} appears to occur with relatively

245   similar frequencies throughout the year. Similar to P_{MD}, P_{WAC} shows an equal distribution all over seasons as expected. Since precipitation is rather uniformly distributed all over the year (see Fig. 2a) wetter than average conditions can occur in any season, and monthly distribution of P_{WAC} cannot be directly linked to the seasonal distribution of high flows. However, wetter conditions (indicated by higher API values) are expected to have different effects on high flows, and a closer examination of the specific condition before every high flow event is necessary. Our findings indicate that extreme precipitation is not the most

250   critical driver of high flows.
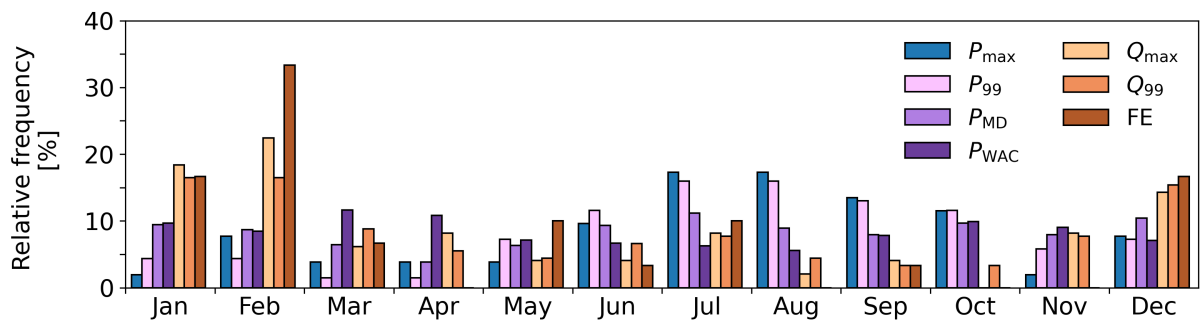
Figure 3. Monthly distribution of annual maximum precipitation (P_{max}), extreme precipitation (P_{99}), multi-day precipitation (P_{MD}) and wet antecedent condition events (P_{WAC}) at the Vaals station, annual maximum discharge (Q_{max}), extremely high flows (Q_{99}) and past flood events (FE) in the Geul.

Figure 4 illustrates the relative frequencies of the introduced indicators (see Table 1) preceding high-flow episodes (i.e., Q_{max}), as described in Sect. 2.3.3. In approximately 75% of the Q_{max} cases, a P_{MD} precedes high-flow events (Fig. 4b), while the corresponding percentage for P_{WAC} is approximately 48% (Fig. 4c). In most cases, P_{WAC} should be followed by P_{MD} in order to generate high flows (similar percentages between P_{WAC} (Fig. 4c) and Compound II (Fig. 4e)). This is also

255   visible in the calculation of the conditional probability of P_{MD} preceding Q_{max} given that P_{WAC} precedes Q_{max} which is approximately 86% (Fig. 4e). In other words, given that P_{WAC} precedes Q_{max}, there is 86 percent chance that P_{MD} will be followed by Q_{max}. The percentages between Compound I and Compound III events (Fig. 4d and 4f) are the same, showing that each time a Q_{max} is preceded by P_{99} it also preceded by P_{MD}. This effect in most cases is caused by the high amount of precipitation that fell at the day of the event or the previous day (definition of P_{99}) which also increases the 4day precipitation

260   (higher than the P_{MD} 95th percentile). P_{99}, Compound I, and Compound III are rare events compared to the other drivers, and there are years in which they are not observed at all (see Table 2). Therefore, it is essential to focus on reverse relative frequencies. In the unique years when a P_{99} event occurs, it is followed by a Q_{max} event in about 37% of those cases, while these numbers are approximately 43% for Compound I and Compound III, respectively (Table 2). This observation suggests that, despite the extremity of extreme precipitation events, they do not always lead to high flows. High-flow events driven by

265   extreme precipitation mostly occur under wet antecedent conditions, as indicated by the similar relative frequencies of P_{99} and

Compound I (Table 2). Our findings emphasize the role of wet antecedent soil moisture conditions and multiday precipitation in driving high flows in the Geul.
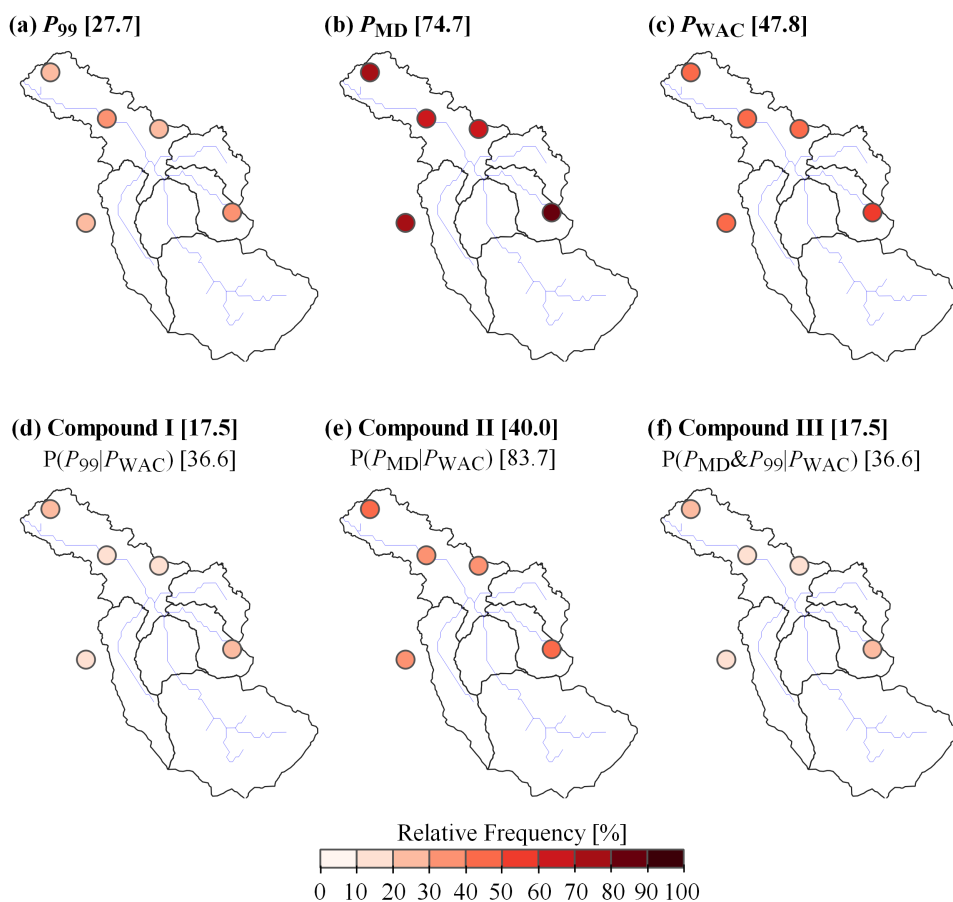
Figure 4. Relative frequencies of $Q_{\max}$ being preceded by (a) extreme precipitation (P_{99}), (b) multi-day precipitation (P_{MD}), (c) wet antecedent conditions (P_{WAC}), (d) extreme precipitation on wet antecedent conditions (Compound I), (e) multi-day precipitation on wet antecedent conditions (Compound II), and (f) extreme and multi-day precipitation on wet antecedent conditions (Compound III), in the total $Q_{\max}$ events (count of a driver leading to $Q_{\max}$ in the $Q_{\max}$ cases divided by the total number of cases). The mean relative frequency (in %) for all rainfall stations is reported in brackets. The mean conditional probabilities of P_{99} and/or P_{MD} preceding $Q_{\max}$ given that P_{WAC} precedes $Q_{\max}$ are also reported per Compound indicator.

Figure 5 shows the $Q_{\max}$ events plotted against their API, including also their preceding precipitation indicators (i.e. P_{99} and P_{MD}) at the Maastricht and Vaals stations. The two stations are selected as an example because in this way the spatial variability of the catchment is considered (the Vaals station is the most upstream station and the station in Maastricht is the most downstream one). P_{99} and/or P_{MD} conditions (green, orange, or purple markers in Fig. 5) that fall under wet conditions (API > 1.5) are classified as compound events (see Table 1). All high flow events appear to happen during normal or wet conditions.

Table 2. General information, averaged for all rainfall stations, regarding the frequency of the different drivers occurring regardless of Q_{max} having occurred, in the Q_{max} period (hydrological years from 1970 to 2021, excluding 1971, 1974 and 1990).

	Number of events (1)	Number of unique years occurred (2)	Mean yearly occurrence (1) / (2)	Number of years followed by Q_{max} (3)	Relative frequency (3) / (2)
P_{99}	64.2	36.4	1.77	13.6	0.37
P_{MD}	873.6	49.0	17.8	36.6	0.75
P_{WAC}	2758	48.4	57.0	23.4	0.49
Compound I	31.4	20.2	1.56	8.6	0.43
Compound II	378.2	44.4	8.52	19.6	0.44
Compound III	31.2	20.0	1.56	8.6	0.43

The absence of green markers in Fig. 5 (only P_{99} events) indicates again that for days preceding Q_{max} the probability of a P_{MD} event given that P_{99} occurs equals one (Pr (P_{MD} | (P_{99} & Q_{max})) = 1). Most extreme events are caused by a combination of P_{99} and P_{MD} or just P_{MD} . Antecedent conditions play also a crucial role in translating precipitation extremes to high flows. We observe that higher API values (higher wet initial conditions) lead to higher peak discharges, especially in compound events where a strong correlation between Q_{max} and API is observed while a very weak correlation between Q_{max} and total event precipitation is reported (see Fig. 5). P_{WAC} makes the difference between a "regular high flow" and a flood event. This is also evident in the initial conditions of the top five floods that occurred in the catchment during the study period (Fig. 5 and Table 3). Details about these events (i.e date of occurrence, different rainfall accumulations, and an estimate of their initial conditions) are presented in Table 3 based on the precipitation records at Maastricht and Vaals (the large discrepancies in rainfall accumulations between the two stations found in Table 3 are caused mainly by the different time interval they include, i.e calendar days for the Maastricht station and 24-hour sums from 8 UTC for the Vaals station, but also the spatial variability).

Table 3. Top five floods that occurred in the catchment during the study period, their rainfall accumulations, and an estimate of their initial conditions based on API. The day with the highest recorded discharge is considered as the date of occurrence of the event. The different precipitation sums (and subsequently API) are based on daily precipitation records at the Maastricht (first value) and Vaals (second value) stations.

No.	Date	24-hour sum [mm]	48-hour sum [mm]	72-hour sum [mm]	30-day before event sum [mm]	API [-]	Initial condition
1	15/07/2021	13.1 / 6.9	53.6 / 80.9	78.0 / 131.5	244.7 / 274.5	3.33 / 3.21	Wet / Wet
2	15/09/1998	9.2 / 28.1	31 / 71.4	48.7 / 74.7	135.5 / 187.2	2.16 / 2.42	Wet / Wet
3	28/02/1987	0.0 / 0.0	13.1 / 13.9	14.5 / 23.1	83.1 / 141.8	1.42 / 1.80	Normal / Wet
4	07/02/1984	22.5 / 10.4	57.1 / 53.2	60.5 / 58.3	131.4 / 170.3	2.24 / 2.20	Wet / Wet
5	22/02/1970	15.0 / 14.1	35.0 / 47.2	38.0 / 53.4	125.4 / 140.5	2.08 / 1.75	Wet / Wet
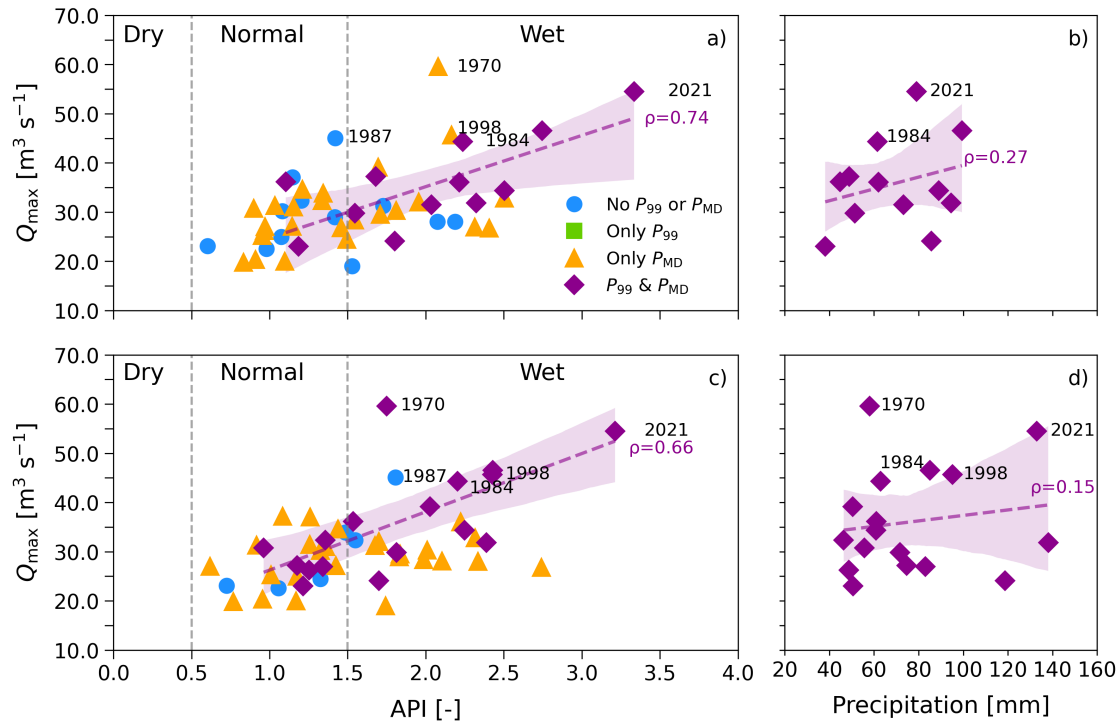
Figure 5. Annual maxima events (Q_{max}) and their Antecedent Precipitation Indices (API) at Maastricht (a) and Vaals (c), including their preceding extreme indicators. Discharge events preceded by P_{99} and/or P_{MD} at the "Wet" classification (API > 1.5) are defined as compound events (see Sect. 2.3.3). The top five floods during the study period are shown with their year of occurrence. The dashed purple line represents the linear fit, using the least squares approach, between the API of the high flow events preceded by P_{99} and P_{MD} and their respective Q_{max} values. The total (four-day) precipitation versus Q_{max} is also presented for these events ((b) Maastricht and (d) Vaals). The shaded area shows the 95% confidence intervals for the fits and the Pearson's correlation coefficients (ρ) are also reported.

We also explore the effect of antecedent precipitation depths on high flows, as an indicator of antecedent catchment wetness.

285 Table 4 reports the correlation coefficients of the $Q_{W,max}$ time series with their k-day (k = 1, 3, 5, 7, 10, 15, 30 and 40) antecedent depths per rainfall station. Results are presented only for the winter half-year as approximately 80% of Q_{max} occurred in this period (Fig. 3). Thus, $Q_{S,max}$ time series contains mainly low discharge values (most of them lower than 20 m^3 s^{-1}, see Fig. 8a) with meaningless correlations. Peak half-year winter discharges in the Geul appear to be closely related to antecedent 10-40 days precipitation depths on wet soils (e.g. correlation coefficient of 0.66 in Vaals for the duration of 15

290 days). The effect of wet antecedent conditions is also reflected here. These results seem reasonable considering the opposing seasonality observed in the catchment (Fig. 3). The July 2021 flood event is consistent with these results as there is evidence that the wetness of the catchments was much higher than usual for the time of the year (see Fig. 5 and Table 3).

Table 4. Correlation coefficients between the winter half-year discharge maxima and their antecedent k-day precipitation depths.

Station	P_{kD} - Winter half-year							
	$k=1$	$k=3$	$k=5$	$k=7$	$k=10$	$k=15$	$k=30$	$k=40$
Vaals	0.44	0.32	0.44	0.40	0.59	0.66	0.56	0.50
Valkenburg	0.30	0.20	0.26	0.28	0.47	0.57	0.52	0.44
Ubachsberg	0.26	0.21	0.25	0.30	0.46	0.56	0.53	0.46
Noorbeek	0.36	0.27	0.36	0.34	0.54	0.61	0.55	0.50
Maastricht	0.24	0.15	0.27	0.27	0.41	0.53	0.49	0.43
Average	**0.32**	**0.23**	**0.31**	**0.31**	**0.49**	**0.59**	**0.53**	**0.47**

3.1.1 Sensitivity of P_{MD} to precipitation duration

In this section, the sensitivity of the P_{MD} probability (and subsequently Compound II and III) preceding high flows with respect
295 to the duration of multi-day precipitation is examined. Table 5 reports the mean relative frequency of Q_{max} events preceded
by the extreme precipitation indicators (see Table 1) for different accumulation periods (i.e P_{MD} using 5, 6, 7, 8, 9 and 10-day
duration). The mean relative probability of P_{MD} decreases by approximately 10% upon increasing the duration from four to
five days. For longer than five-day durations the P_{MD} frequency preceding high flows remains relatively stable. The mean
relative frequencies of Q_{max} preceded by Compound II and III events show a stable pattern irrespective of the selected P_{MD}
300 duration. Overall, we observe that irrespective of the selected duration, our results remain stable. This is also evident from the
non-sensitive Compound II probabilities.

Table 5. Mean relative frequencies for all stations of high flow events preceded by the defined extreme precipitation indicators for different
accumulation periods (see Fig. 4).

P_{MD} duration	P_{99} [%]	P_{MD} [%]	P_{WAC} [%]	Compound I [%]	Compound II [%]	Compound III [%]
4-day		74.7			38.4	17.5
5-day		64.5			39.6	17.5
6-day		64.5			39.6	17.5
7-day	27.7	61.6	47.8	17.5	39.6	17.1
8-day		57.5			38.3	17.1
9-day		60.8			41.6	17.5
10-day		58.4			39.2	16.3

A 4-day duration was selected for the definition of an P_{MD} event as we wanted to ensure that the 95th percentile was higher
than the 99th percentile of P_{99}. In this way usually more than two days of precipitation are required to exceed the four-day 95th

percentile and cause P_{MD}. In extreme 24-hour events this threshold could be exceeded, however, with increasing P_{MD} duration

305 the difference between the 95th P_{MD} percentile and the 99th P_{99} percentile becomes larger (since the 95th P_{MD} percentile is much higher). However, in the way we defined P_{99} (two days interval) we observed that the P_{99} events preceding a $Q_{\max}$ usually coincided with also P_{MD}. This doesn't affect the results. P_{MD}, which cannot alone cause P_{99}, mainly lead to $Q_{\max}$. Then depending mainly on the wet conditions, the extreme events are translated into floods.

3.2 Trend analysis

310 #### 3.2.1 Flood driver trends

Figure 6 illustrates the multi-temporal trend analysis for several precipitation indices for the Vaals station, for half-year periods, as an example. The multi-temporal analysis for Vaals, which has a record from 1952 to 2021, results in 861 trends. In the winter half-year statistically significant increasing trends are found for the longest periods in all indices at Vaals. However, a decreasing, mainly insignificant, pattern is visible in the recent past (trends starting after the 1980s). In summer (Fig. 6b)

315 negative trends are visible for the longest periods, while this changes to positive trends in the recent past for $k \leq 5$ days. Summer trends for $k > 5$ days are rather mixed: generally insignificant trends, with shifts between positive and negative tendencies. For the full multi-temporal analysis per index and station, please refer to the supplementary material.

Figure 7 shows the consistency of statistically significant trends in each precipitation index per rainfall station. In winter only increasing trends are visible, with the exception of the $P_{15\mathrm{D}}$ index at Ubachsberg. The decreasing tendency in the recent

320 past detected at Vaals is very strong and statistically significant at Ubaschberg for most indices (Fig. S3 in supplement), which causes this inconsistent decrease. Consistent and strongly consistent increases are observed in at least one station per index. In the index $P_{7\mathrm{D}}$ four out of five stations show consistent or strongly consistent increases. For $k \leq 10$ days most stations have strongly consistent or consistent upward directions. With increasing k (15,..,40 days) the increase becomes weaker (inconsistent) for the majority of the stations, however still two out of five stations (located inside the catchment) show increases.

325 Indices for $k \leq 10$ days are strongly consistently increasing, while for $k > 10$ days a consistent increase is visible in the station Valkenburg. In addition, three out of five stations show strongly consistent or consistent increasing trends in the indices P_{95} and P_{MD}. Overall, the trend analysis in winter for the Geul catchment shows a consistent increase of very wet days (P_{95}) and maximum k-day precipitation sums. The rise in severe precipitation is caused mostly by more rain on already wet days. Multi-day precipitation extremes are consistently increasing. This is a crucial finding, as the effects of prolonged heavy storms

330 in combination with wet antecedent conditions appear to be the dominant flood drivers in the Geul catchment.

Trends in summer periods show variability across the different stations. The majority of the summer half-year k-day and P_{95} indices are subject to inconsistent trends. Most stations show generally insignificant trends, with changes between positive and negative tendencies. The only consistent trends are mainly increasing and are found at the Valkenburg station for $k = 5, 7,$ 10, 15 days, at Ubachsberg for $k = 7$ days, and at Maastricht (i.e P_{MD}). In addition, the $P_{30\mathrm{D}}$ and P_{95} indices at Maastricht

335 show strong and statistically significant increasing trends in the majority of tested cases resulting in weakly consistent trends. As mentioned, despite the fact that the difference between significant increasing and decreasing trends in the summer half-year
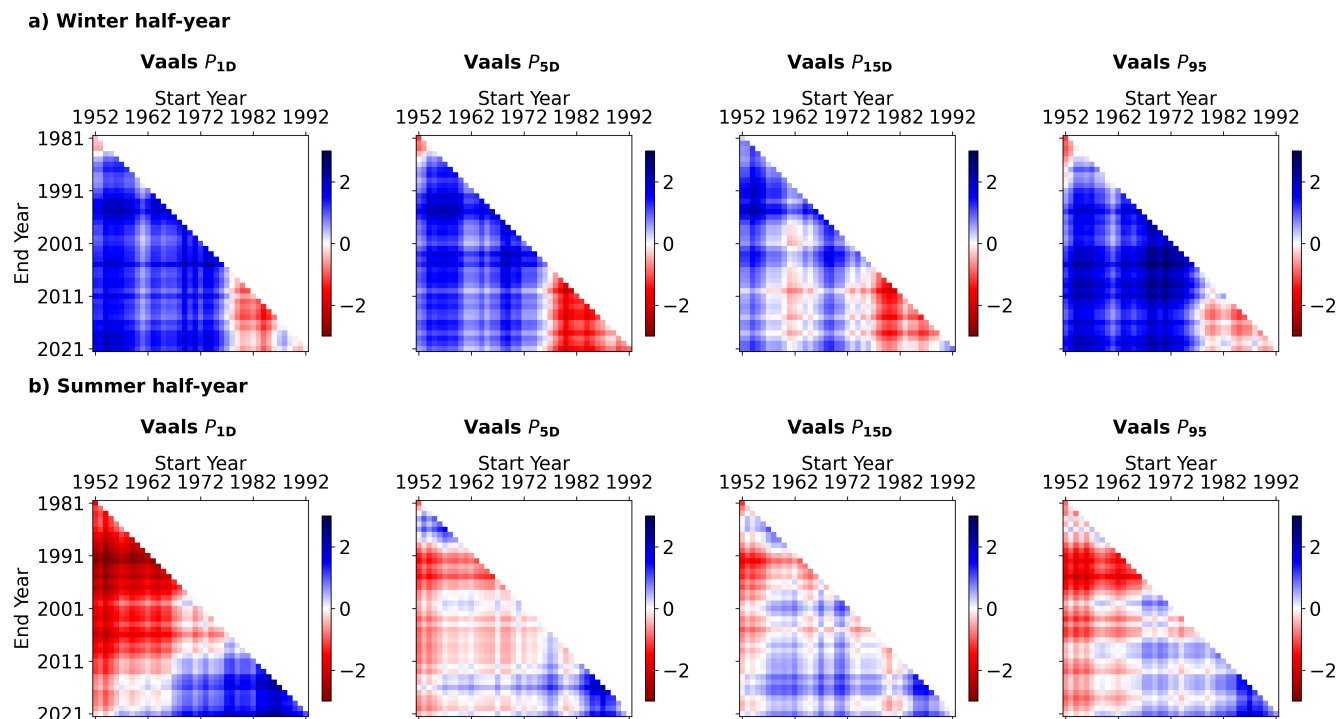
Figure 6. Multi-temporal trend analysis for P_{1D}, P_{5D}, P_{15D} and P_{95} at Vaals for (a) winter half-year and (b) summer half-year. Each pixel presents a fixed single period (minimum window length of 30 years) of start and end year. For each period the M-K test is applied, and the color indicates the Z-statistic value of the test (the same definitions apply to the subsequent figures). Blue colors indicate increasing trends and red downward ones. The darker the color, the more significant the trend. Statistically significant trends are considered those with Z-statistic values higher than 1.28 (or smaller than -1.28 for downward trends) corresponding to the defined significance level of 0.2 (see Sect. 2.4).

is not clear, the statistically significant increasing trends in the recent past, mainly for $k \leq 3$ days, are strong and should be taken into account (Fig. S6 - S10 in supplement). In addition, the consistent increasing trends at Valkenburg reveal a direction towards more wet conditions in the summer half-year.

340 **3.2.2 Discharge trends**

The results of the multi-temporal analysis for the $Q_{W,max}$ and $Q_{S,max}$ time series are shown in Fig. 8. It can be observed that the maximum flows show variability over the two half-year periods. Strong increasing trends are found in the longest periods for the winter half-year but this seems to have changed in the recent past to statistically insignificant decreasing tendencies. Overall, the increase in the $Q_{W,max}$ is consistent. This pattern is in agreement with the extreme precipitation trends in the area for winter, as large similarities are observed in terms of magnitudes, directions and variabilities. For example, $Q_{W,max}$ trends

345
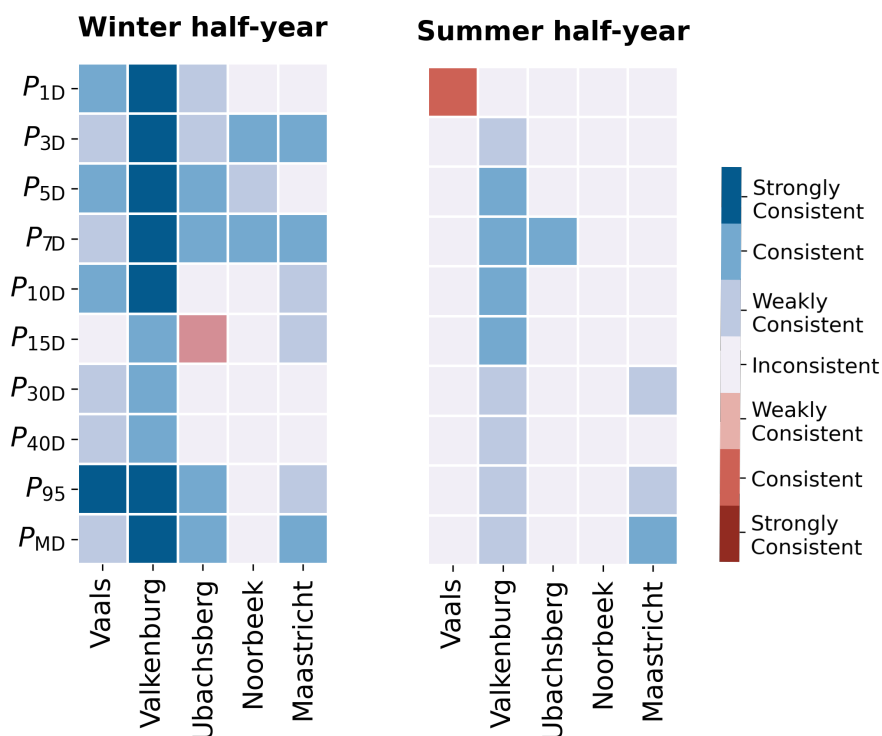
Figure 7. Temporal consistency of precipitation trend indices for winter and summer half-years. Blue colors indicate upward trends while red colors indicate downward trends.

variability is quite similar to P_{95} index in winter at Vaals (see Fig. 6a): statistically stronger increasing trends in longer periods (from 1970 to 2021) with a weak decreasing direction in the recent past (trends starting from the 1980s).

Mixed and non statistically significant trends are observed in the summer half-year (Fig. 8c), as expected, considering that the trends in extreme precipitation in the same period are inconsistent and their strength is (statistically) insignificant. $Q_{\mathrm{S,max}}$

350 trends shift between negative and positive tendencies in similar, for some cases, periods with the extreme summer precipitation, however this match is not so clear as in the winter period. The increasing direction of extreme precipitation in the recent past for summer starts becoming visible also in the $Q_{\mathrm{S,max}}$ direction (see positive values for trends starting after 1985). In general, in summer the effect of the considerable increase in evaporation in the area (Tsiokanos, 2022) in combination with the large soil moisture deficits should be taken into account when translating extreme precipitation to extreme streamflows, and subsequently

355 discussing correspondences and differences between discharge and precipitation trends.
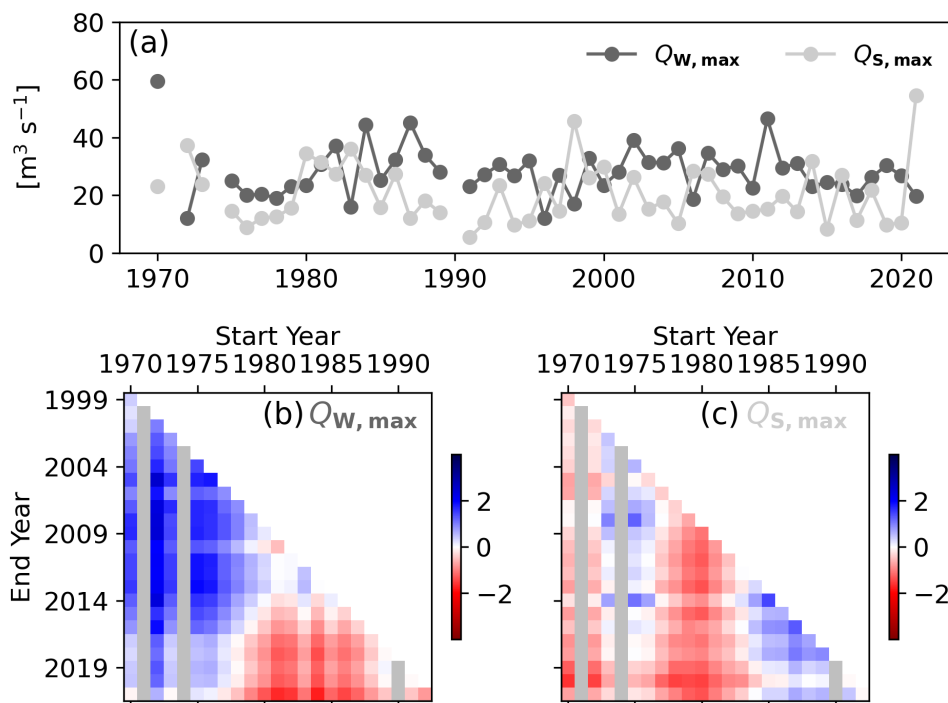
Figure 8. Half-year yearly maxima time series (a) and multi-temporal trend analysis for (b) winter half-year yearly maxima ($Q_{W,max}$) and (c) summer half-year yearly maxima ($Q_{S,max}$). The gray stripes in the heatmaps indicate the excluded hydrological years (i.e. 1971, 1974 and 1990).

4 Discussion

4.1 Data uncertainty

Records of 24-hour precipitation are used that come from the KNMI manual rain gauge network. The used precipitation time resolution may be considered low for flood analysis, however the response time (i.e. longer than a day, see Sect. 2.1) of the
360 catchment allows the application of this resolution. In addition, the main goal of this paper is to investigate the role of P_{99}, P_{MD}, and P_{WAC} as potential flood drivers. The use of 24-hour resolution can affect the defined P_{99}, while the applied resolution does not have a major impact on the definitions and meaning of P_{MD} and P_{WAC}. For this reason, allowances were made in the way we define a P_{99} day (i.e. precipitation amount at the same or previous day of the high flow event; see Sect. 2.3.3).

Long precipitation time series may have been influenced by instrumental modifications and station relocations throughout the
365 recording period. As mentioned in Sect. 2.2, the data are considered to be of high quality, as KNMI performs regular quality tests. In addition to that, two homogeneity tests were applied to monthly sums. In general, it is assumed that the analyzed precipitation time series in this research are not affected by instrumental and location alterations, so the trends that are found can be attributed to climate and not to human interventions.

It must be acknowledged that the produced discharge results are subject to significant uncertainty (Di Baldassarre and
370 Montanari, 2009). Estimations during extremely high flows are very inaccurate. For example, the recorder discharge in July
2021 flood was 55 m^{3}s^{-1}, while it is estimated that it exceeded 80 m^{3}s^{-1} (van Heeringen et al., 2022). However, our main
findings about the role of P_{WAC} and P_{MD} in generating high flows remain valid. In addition, periods of transition, changes
in gauge position, equipment, and monitoring frequencies, and stage-discharge relations can cause sudden variations in flow
rates. These changes can be more visible in mean flow trends where the values are low in contrast to high flows used in this
375 paper. The long-term measurements of the station Meerssen at the outlet of the catchment are considered reliable in terms
of homogeneity (Agor, 2003). The high flow trends are found to be similar to the directions and significance of the extreme
precipitation trends, indicating that the results are likely not affected.

4.2 Implications

It is found for the Geul that extreme daily precipitation is not solely a flood driver. Wet antecedent soil conditions are a crucial
380 factor determining the probability of flooding. In this respect, the finding that heavy prolonged precipitation is the main high
flow mechanism in the Geul seems reasonable, as multi-day precipitation can be used also as a proxy for heavy precipitation
occurring on wet antecedent circumstances (Nanditha and Mishra, 2022). Most of the flood events are observed in winter
periods, when the catchment tends to be very wet, with shallow groundwater tables. In summer periods most of the extreme
(intense) precipitation events are not translated to high flow peaks, due to large soil moisture deficits. The most devastating
385 flood in the area (i.e. July 2021) was aggravated by rainfall events in preceding days and weeks. The role of wet antecedent
(soil) conditions in driving floods is well established, however, the focus tends to be on larger catchments (Wasko et al., 2020).
Information about the initial (wet) conditions of the catchment is deemed essential, particularly for flood forecasting, since the
local water authority currently does not monitor soil moisture. In addition, the geology of the Geul can significantly control
the runoff response, as there is a thick unsaturated chalk zone that can store much water (Klein, 2022). The (geo)hydrological
390 properties and characteristics of the catchments should receive more attention in the flood forecasting system (Zanon et al.,
2010; Douinot et al., 2022). Our findings are also expected to help in the understanding of flood mechanisms in other lowland
or chalk catchments around the world. In addition, the followed event-based approach can be exploited in other catchments
to examine the relative role of wet antecedent soil moisture conditions and precipitation characteristics preceding high flows,
especially in areas where (long-term) soil moisture data are not available.

395 The statistical results obtained in Sect. 3.2.1 demonstrate some intriguing variations in the Geul catchment's precipitation
regimes across the studied periods. The most notable change is the consistent and strong increase in critical precipitation
during the winter half-year. The rise in severe precipitation is caused mostly by more rain on already wet days. This is a crucial
finding as prolonged rainfall events have impacted the catchment and caused floods mainly in winter. Although it cannot be
concluded that climate change had a significant impact on the July 2021 flood event in the Geul region, as there are no apparent
400 consistent patterns in most summer precipitation trends, a concerning increasing direction in the recent past (mainly after the
1980s) is visible. This finding is important as it shows that, except for the intense showers in summer, the effects of heavy
storms in combination with wet antecedent conditions should be also taken into account. At the same time, it is critical to

consider the substantial increase in summer potential evaporation rates (due to increases in temperature and radiation) in the area (Tsiokanos, 2022) that may lead to soil moisture deficits, when translating extreme precipitation events into potential

405 extreme flows. According to the recently published KNMI scenarios wetter winters and increased extreme summer showers are projected for the Netherlands (KNMI, 2023). These projections suggest that the number of heavy showers with significant precipitation is expected to rise, with a shift from light to heavier (more rain falls from the shower) and more intense (more rain falls in a certain time) showers (KNMI, 2023). These climate scenarios are in line with the trends found in this study. Overall, the long-term trends of the critical precipitation are also visible in the runoff patterns. Thus, climate change should

410 be taken seriously into account in the area and should be incorporated into flood designs, considering also the effects of agro-economic developments, such as land-use changes. Our findings from the precipitation and discharge trend analyses can serve as a valuable reference for assessing the impact of climate change on precipitation and discharge patterns in other regions than the Geul as well. In addition, the use of a multi-temporal approach, including the consistency criteria, appears useful and is recommended for identifying variability, recent directions but also long-term trends.

415 **5 Conclusions**

We used an event-based approach to detect the main flood drivers in the Geul river catchment and a multi-temporal trend analysis to investigate their temporal variability and consistency. Our results show that heavy multi-day precipitation is the prominent high flow driver in the catchment, as it precedes high flow events approximately 75% of time (using a 4-day precipitation duration) (Fig. 4). Wet antecedent conditions play a crucial role in translating extreme events into extreme flows and

420 make the difference between a "regular high flow" and a flood event. Extreme (24-hour) precipitation, without wet antecedent conditions, which appears mainly in summer, has never led solely to floods in the past (Fig. 5 and Table 3). The joint probability of heavy (prolonged) rainfall and wet initial conditions (which can be seen as a compound event) determines the chances of flooding. As a result, prolonged heavy rainfall and wet antecedent wetness appear to be the main high-flow generating factors and should be used as flood indicators, rather than extreme precipitation alone. Critical precipitation (precipitation that

425 leads to floods) shows a consistent increase in the winter half-year, a period in which more than 70% of extremely high flows have occurred historically. Heavy prolonged storms in combination with wet antecedent conditions can cause large flooding and these conditions are becoming more frequent during winters. This rise is also reflected in the winter half-year maximum discharges, which are increasing in terms of magnitude. Although the majority of precipitation and flow trends do not exhibit consistent patterns in the summer half-year, a notable and concerning upward direction has become evident in the recent past.

430 This observation underscores the necessity to account for compound events' effects in addition to intense summer showers. The extreme flood event of July 2021, along with the observed increase in flood drivers, emphasizes the importance of incorporating compound events into flood risk assessment.

Data availability. Precipitation data used in this study were obtained from the Royal Netherlands Meteorological Institute (KNMI). Time series for the manual rain gauge network can be downloaded from https://www.knmi.nl/nederland-nu/klimatologie/monv/reeksen and for the
435 meteorological station at Maastricht from https://daggegevens.knmi.nl/klimatologie/daggegevens. Discharge time series at Meerssen were provided by the water authority Waterschap Limburg and should be requested via them.

Author contributions. All authors contributed to the study conception and design. AT conducted all the analyses. AT prepared the manuscript, and all co-authors contributed to the content and improvement of the manuscript.

Competing interests. The authors declare that they have no conflict of interests.

440 *Acknowledgements.* This research was financially supported by the EMfloodResilience project, which was carried out within the context of Interreg V-A Euregio MeuseRhine and is partially funded by the European Regional Development Fund. The authors would like to thank the Royal Netherlands Meteorological Institute (KNMI) and the water authority Waterschap Limburg for providing all the data used in this work. We would also like to thank Deltares for supporting parts of this research.

References

445 Agor, M. L. C.: Assessment of the long-term rainfall runoff relation of the Geul catchment, Master's thesis, UNESCO–IHE Institute for Water Education, The Netherlands, 2003.

Alexandersson, H.: A homogeneity test applied to precipitation data, Journal of Climatology, 6, 661–675, 1986.

Alexandersson, H. and Moberg, A.: Homogenization of Swedish temperature data. Part I: Homogeneity test for linear trends, International Journal of Climatology: A Journal of the Royal Meteorological Society, 17, 25–34, 1997.

450 Andrés-Doménech, I., García-Bartual, R., Montanari, A., and Marco, J.: Climate and hydrological variability: the catchment filtering role, Hydrology and Earth System Sciences, 19, 379–387, 2015.

Asselman, N., van Heeringen, K.-J., de Jong, J., and Geertsema, T.: Juli 2021 overstroming en wateroverlast in Zuid-Limburg: Eerste bevindingen voor Valkenburg, Geulmonding, Roermonding en Eygelshoven, Tech. rep., Deltares, report 11207700-000-ZWS-0019, The Netherlands, https://www.waterschaplimburg.nl/publish/pages/7013/juli_2021_overstroming_en_wateroverlast_in_zuid-limburg.pdf, 2022.

455 Berghuijs, W. R., Harrigan, S., Molnar, P., Slater, L. J., and Kirchner, J. W.: The relative importance of different flood-generating mechanisms across Europe, Water Resources Research, 55, 4582–4593, 2019.

Bertola, M., Viglione, A., Lun, D., Hall, J., and Blöschl, G.: Flood trends in Europe: are changes in small and big floods different?, Hydrology and Earth System Sciences, 24, 1805–1822, 2020.

Blöschl, G., Hall, J., Parajka, J., Perdigão, R. A., Merz, B., Arheimer, B., Aronica, G. T., Bilibashi, A., Bonacci, O., Borga, M., et al.:
460 Changing climate shifts timing of European floods, Science, 357, 588–590, 2017.

Blöschl, G., Hall, J., Viglione, A., Perdigão, R. A., Parajka, J., Merz, B., Lun, D., Arheimer, B., Aronica, G. T., Bilibashi, A., et al.: Changing climate both increases and decreases European river floods, Nature, 573, 108–111, 2019.

Brauer, C., van der Velde, Y., Teuling, A., and Uijlenhoet, R.: The hupsel brook catchment: Insights from five decades of lowland observations, Vadose Zone Journal, 17, 1–8, 2018.

465 Buishand, T. A.: Tests for detecting a shift in the mean of hydrological time series, Journal of Hydrology, 73, 51–69, 1984.

Buishand, T. A., De Martino, G., Spreeuw, J., and Brandsma, T.: Homogeneity of precipitation series in the Netherlands and their trends in the past century, International Journal of Climatology, 33, 815–833, 2013.

Di Baldassarre, G. and Montanari, A.: Uncertainty in river discharge observations: a quantitative analysis, Hydrology and Earth System Sciences, 13, 913–921, 2009.

470 Do, H. X., Westra, S., and Leonard, M.: A global-scale investigation of trends in annual maximum streamflow, Journal of hydrology, 552, 28–43, 2017.

Douinot, A., Iffly, J. F., Tailliez, C., Meisch, C., and Pfister, L.: Flood patterns in a catchment with mixed bedrock geology and a hilly landscape: identification of flashy runoff contributions during storm events, Hydrology and Earth System Sciences, 26, 5185–5206, 2022.

Dunn, R. J., Alexander, L. V., Donat, M. G., Zhang, X., Bador, M., Herold, N., Lippmann, T., Allan, R., Aguilar, E., Barry, A. A., et al.:
475 Development of an updated global land in situ-based data set of temperature and precipitation extremes: HadEX3, Journal of Geophysical Research: Atmospheres, 125, e2019JD032 263, 2020.

Garg, S. and Mishra, V.: Role of extreme precipitation and initial hydrologic conditions on floods in Godavari river basin, India, Water Resources Research, 55, 9191–9210, 2019.

Haan, C. T.: Statistical methods in hydrology, The Iowa State Press, Ames, 2 edn., 2002.

480 Hannaford, J., Buys, G., Stahl, K., and Tallaksen, L.: The influence of decadal-scale variability on trends in long European streamflow records, Hydrology and Earth System Sciences, 17, 2717–2733, 2013.

Hannaford, J., Mastrantonas, N., Vesuviano, G., and Turner, S.: An updated national-scale assessment of trends in UK peak river flow data: how robust are observed increases in flooding?, Hydrology Research, 52, 699–718, 2021.

Hussain, M. and Mahmud, I.: pyMannKendall: a python package for non parametric Mann Kendall family of trend tests., Journal of Open
485 Source Software, 4, 1556, 2019.

Journée, M., Goudenhoofdt, E., Vannitsem, S., and Delobbe, L.: Quantitative rainfall analysis of the 2021 mid-July flood event in Belgium, Hydrology and Earth System Sciences, 27, 3169–3189, https://doi.org/10.5194/hess-27-3169-2023, 2023.

Kendall, M. G.: Rank Correlation Methods: By Maurice G. Kendall., Hafner, 1955.

Klein, A.: Hydrological Response of the Geul Catchment to the Rainfall in July 2021, Master's thesis, Delft University of Technology, The
490 Netherlands, http://resolver.tudelft.nl/uuid:ee25d687-70af-4aca-ae41-78e3f83943bf, 2022.

Klein Tank, A., Wijngaard, J., Können, G., Böhm, R., Demarée, G., Gocheva, A., Mileta, M., Pashiardis, S., Hejkrlik, L., Kern-Hansen, C., et al.: Daily dataset of 20th-century surface air temperature and precipitation series for the European Climate Assessment, International Journal of Climatology: A Journal of the Royal Meteorological Society, 22, 1441–1453, 2002.

KNMI: KNMI'23 klimaatscenario's voor Nederland, Tech. rep., Royal Netherlands Meteorological Institute (KNMI), https://cdn.knmi.nl/
495 system/data_center_publications/files/000/071/901/original/KNMI23_klimaatscenarios_gebruikersrapport_23-03.pdf, 2023.

Kreienkamp, F., Philip, S. Y., Tradowsky, J. S., Kew, S. F., Lorenz, P., Arrighi, J., Belleflamme, A., Bettmann, T., Caluwaerts, S., Chan, S. C., et al.: Rapid attribution of heavy rainfall events leading to the severe flooding in Western Europe during July 2021, https://www.worldweatherattribution.org/wp-content/uploads/Scientific-report-Western-Europe-floods-2021-attribution.pdf, 2021.

Lupikasza, E.: Spatial and temporal variability of extreme precipitation in Poland in the period 1951–2006, International Journal of Clima-
500 tology: A Journal of the Royal Meteorological Society, 30, 991–1007, 2010.

Łupikasza, E. B., Hänsel, S., and Matschullat, J.: Regional and seasonal variability of extreme precipitation trends in southern Poland and central-eastern Germany 1951–2006, International Journal of Climatology, 31, 2249–2271, 2011.

Mann, H. B.: Nonparametric tests against trend, Econometrica: Journal of the econometric society, pp. 245–259, 1945.

Marchi, L., Borga, M., Preciso, E., and Gaume, E.: Characterisation of selected extreme flash floods in Europe and implications for flood
505 risk management, Journal of Hydrology, 394, 118–133, 2010.

Mohr, S., Ehret, U., Kunz, M., Ludwig, P., Caldas-Alvarez, A., Daniell, J. E., Ehmele, F., Feldmann, H., Franca, M. J., Gattke, C., Hundhausen, M., Knippertz, P., Küpfer, K., Mühr, B., Pinto, J. G., Quinting, J., Schäfer, A. M., Scheibel, M., Seidel, F., and Wisotzky, C.: A multi-disciplinary analysis of the exceptional flood event of July 2021 in central Europe – Part 1: Event description and analysis, Natural Hazards and Earth System Sciences, 23, 525–551, https://doi.org/10.5194/nhess-23-525-2023, 2023.

510 MunichRe: Hurricanes, cold waves, tornadoes: Weather disasters in USA dominate natural disaster losses in 2021, Europe: Extreme flash floods with record losses, https://www.munichre.com/en/company/media-relations/media-information-and-corporate-news/media-information/2022/natural-disaster-losses-2021.html, 2022.

Murphy, C., Wilby, R. L., Matthews, T. K., Thorne, P., Broderick, C., Fealy, R., Hall, J., Harrigan, S., Jones, P., McCarthy, G., et al.: Multi-century trends to wetter winters and drier summers in the England and Wales precipitation series explained by observational and sampling
515 bias in early records, International Journal of Climatology, 40, 610–619, 2020.

Nanditha, J. and Mishra, V.: Multiday Precipitation Is a Prominent Driver of Floods in Indian River Basins, Water Resources Research, 58, e2022WR032 723, 2022.

Schär, C., Ban, N., Fischer, E. M., Rajczak, J., Schmidli, J., Frei, C., Giorgi, F., Karl, T. R., Kendon, E. J., Tank, A. M. K., et al.: Percentile indices for assessing changes in heavy precipitation events, Climatic Change, 137, 201–216, 2016.

520 Sharma, A., Wasko, C., and Lettenmaier, D. P.: If Precipitation Extremes Are Increasing, Why Aren't Floods?, Water Resources Research, 54, 8545–8551, 2018.

Slager, K.: Gevolgen overstromingen Limburg: Inventarisatie en duiding, Tech. rep., Deltares, report 11207700-007-ZWS-0011, The Netherlands, https://publications.deltares.nl/11207700_007_0011.pdf, 2023.

Sperna-Weiland, F., Hegnauer, M., Bouaziz, L., and Beersma, J.: Implications of the KNMI'14 Climatescenarios for the Discharge of the

525 Rhine and Meuse: Comparison with Earlier Scenario Studies, Deltares, 2015.

Squintu, A. A., van der Schrier, G., van den Besselaar, E., van der Linden, E., Putrasahan, D., Roberts, C., Roberts, M., Scoccimarro, E., Senan, R., and Klein Tank, A.: Evaluation of trends in extreme temperatures simulated by HighResMIP models across Europe, Climate Dynamics, 56, 2389–2412, 2021.

Task Force Fact Finding hoogwater 2021: Hoogwater 2021: Feiten en Duiding, Tech. rep., Expertise Netwerk Waterveiligheid, https://doi.

530 org/10.4233/uuid:06b03772-ebe0-4949-9c4d-7c1593fb094e, 2021.

Thewissen, A.: Flood event of July 2021: How extreme were the floods in the Ahr, Vesdre and Geul?, Master's thesis, Delft University of Technology, The Netherlands, http://resolver.tudelft.nl/uuid:a7436524-e11b-4922-8637-6a74a1868f04, 2022.

Tramblay, Y., Villarini, G., El Khalki, E. M., Gründemann, G., and Hughes, D.: Evaluation of the drivers responsible for flooding in Africa, Water Resources Research, 57, e2021WR029 595, 2021.

535 Tsiokanos, A.: Investigation of the Impacts of Climate Variability and Land Use Changes on the Hydrology of the Geul River Catchment, Master's thesis, Delft University of Technology, The Netherlands, http://resolver.tudelft.nl/uuid:bf03fedd-88a1-4cb0-a72a-1487dcf56402, 2022.

Tu, M.: Assessment of the effects of climate variability and land use change on the hydrology of the Meuse river basin, PhD dissertation, UNESCO-IHE Institute for Water Education, The Netherlands, 2006.

540 van der Deijl, E.: Validatie hoogwater Maas juli 2021, Tech. rep., Deltares, report 11208053-002-ZWS-0006, The Netherlands, https://publications.deltares.nl/11208053_002_0006.pdf, 2023.

van Heeringen, K.-J., Asselman, N., Overeem, A., Beersma, J., and Philip, S.: Analyse overstroming Valkenburg. Watersysteemevaluatie Waterschap Limburg, Tech. rep., Deltares, report 11207700-000-ZWS-0014, The Netherlands, https://www.waterschaplimburg.nl/actueel/nieuws/@7103/resultaten-case-studies-vier/, 2022.

545 Wasko, C. and Nathan, R.: Influence of changes in rainfall and soil moisture on trends in flooding, Journal of Hydrology, 575, 432–441, 2019.

Wasko, C., Nathan, R., and Peel, M. C.: Changes in antecedent soil moisture modulate flood seasonality in a changing climate, Water Resources Research, 56, e2019WR026 300, 2020.

Woldemeskel, F. and Sharma, A.: Should flood regimes change in a warming climate? The role of antecedent moisture conditions, Geophys-

550 ical Research Letters, 43, 7556–7563, 2016.

Yang, L., Yang, Y., Villarini, G., Li, X., Hu, H., Wang, L., Blöschl, G., and Tian, F.: Climate more important for Chinese flood changes than reservoirs and land use, Geophysical Research Letters, 48, e2021GL093 061, 2021.

Zanon, F., Borga, M., Zoccatelli, D., Marchi, L., Gaume, E., Bonnifait, L., and Delrieu, G.: Hydrological analysis of a flash flood across a climatic and geologic gradient: The September 18, 2007 event in Western Slovenia, Journal of Hydrology, 394, 182–197, 2010.